HIGH RESOLUTION MEDICAL ACOUSTIC VASCULAR IMAGING USING FREQUENCY DOMAIN INTERFEROMETRY

Hirofumi Taki, Tomoki Kimura, Takuya Sakamoto, Toru Sato
Graduate School of Informatics, Kyoto University
Yoshida-honmachi, Sakyo-ku, Kyoto 606-8501
Japan
taki@sis.i.kyoto-u.ac.jp

ABSTRACT
We employed frequency domain interferometry (FDI) for medical acoustic vascular imaging to detect multiple targets with high range resolution. The phase of each frequency component of an echo varies with the frequency, and we can estimate target intervals from the phase variance. This processing technique is generally used in radar imaging. When the interference within a range gate is coherent, the cross correlation between the desired signal and the coherent interference signal is nonzero. Since Capon method works under the guiding principle of output power minimization, the desired signal is canceled by a coherent interference signal. Therefore, we utilize the frequency averaging to suppress the correlation of the coherent interference. The results of computational simulations using a pseudo echo signal showed that Capon method with a frequency averaging technique using a single reference wave presents a higher range resolution than that using a conventional method. In the experimental study the range resolution of FDI with Capon method using a single reference wave deteriorates severely because we approximated the auto-correlation function of the echo to the cross-correlation function of the echo and the reference signal. Therefore we proposed FDI with Capon method using multiple optimized reference waves. The proposed target detection method using optimized reference waves had higher range resolution than that using a single reference wave, and could distinct two target boundaries that lied 0.05mm apart experimentally.

KEY WORDS
medical acoustic imaging, vascular imaging, frequency domain interferometry, Capon, frequency averaging, and coherent interferences

1. Introduction

Medical acoustic imager with high range resolution is desired significantly to diagnose carotid artery atherosclerosis. Several methods have been proposed for the improvement of range resolution[1-4]; however, it is still technical challenging. Kudo et al.[5] reported another imaging technique, using the frequency spectrum of a radiofrequency echo signal to measure the wall thickness of the carotid artery. The theory is based on the spectrum change caused by target interval. The technique permits only the case two targets exist in a range. Since the 1960's adaptive beamforming techniques have been employed to reduce the effect of the noise and non-desired signal's contribution, resulting in high-resolution imaging. In 1969 Capon[6] proposed an adaptive beamforming method for radio astronomy. Shan and Kailath[7] introduced a spatial averaging technique into the Capon method to suppress the coherent interference. Mann and Walker[8] employed the Capon method on experimental data of a single point-target and confirmed the improvement of spatial resolution. In medical acoustic imaging Sasso and Cohen-Bacrie[9] investigated the improvement of spatial resolution experimentally using the Capon method with spatial averaging. In this paper, we introduced the Capon method with spatial averaging techniques into frequency domain interferometry (FDI), which has been developed for radar imaging, to realize a high range resolution medical acoustic imager. The proposed method can estimate multiple targets position within a range gate. This method is suitable for medical acoustic imaging requiring high range resolution, such as carotid artery wall imaging.

2. High Resolution Imaging with FDI

2.1 The processing method of FDI

Our previous work estimated the interval of multiple targets within a range gate using the phases of signals at different frequencies[10]. The phase difference between two signals from different targets is proportional to the product of the frequency and the target interval. Thus the phase difference varies with the frequency of a signal, as depicted in Fig. 1. The variance of the phase difference between two signals at different frequencies is proportional to the product of the frequency difference and the target interval. Therefore we can estimate the target interval utilizing the variance of the phase difference.

To obtain a range profile, we calculate correlation values between signals at different frequencies. The signals are similarly expressed in a vertical form as follows.
The output of an imager, y, is given by

$$y = \mathbf{X}^{\mathrm{T}}\mathbf{W}^{*} = \mathbf{W}^{\dagger}\mathbf{X}, \quad (1)$$

$$\mathbf{X} = \begin{bmatrix} X_1 & X_2 & \cdots & X_N \end{bmatrix}^{\mathrm{T}}, \quad (2)$$

$$\mathbf{W} = \begin{bmatrix} \mathbf{W}_1, \cdots, \mathbf{W}_N \end{bmatrix}^{\mathrm{T}}, \quad (3)$$

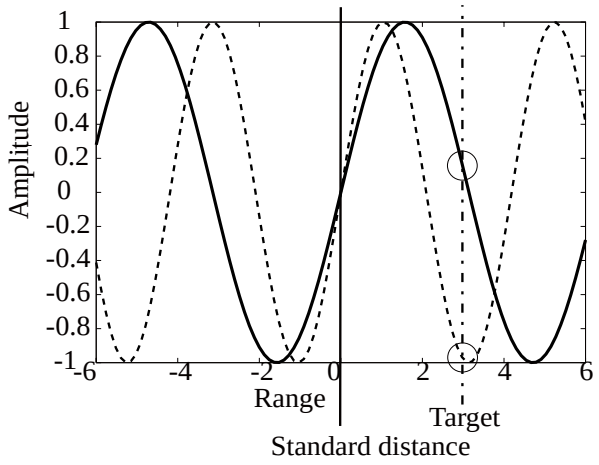

Fig. 1 Schema of the phases of the signals at different frequency.

where $\mathbf{X}$ is a signal expressed by a set of frequency components in a vertical form, $\mathbf{W}$ is a weighting function, and N is the number of frequency component samples of the signal. The output power P is given by

$$P = E[yy^{*}] = \mathbf{W}^{\dagger}\mathbf{R}\mathbf{W}, \quad (4)$$

$$\mathbf{R} = E[\mathbf{X}\mathbf{X}^{\dagger}], \quad (5)$$

where $E[]$ denotes the expectation and $\mathbf{R}$ is the correlation matrix of the input signals at each frequency. We then integrate the correlation values with the weighting function for phase correction.

2.2 Capon method

The beamformer method scans all distances within a range gate. When multiple targets exist within a range gate, the resolution of the beamformer method deteriorates because of the interference by the targets at other positions. Therefore we used the Capon method, minimizing the contribution from other distances subject to a constant response at a desired distance[6]. This problem is expressed as follows[11];

$$\min \quad P(r) \quad \text{subject to} \quad \mathbf{C}^{\dagger}\mathbf{W} = 1, \quad (6)$$

$$\mathbf{C} = \left[e^{\mathrm{j}k_1 r}, \cdots, e^{\mathrm{j}k_N r} \right]^{\mathrm{T}}, \quad (7)$$

where r is the range, k_j is wavenumber when frequency number is j, $\mathbf{C}$ is the constraint vector. They can be solved owing to Lagrange multiplier methods. The solution to eqs. (6) and (7) is given by

$$P_{\mathrm{Cap}}(r) = \frac{1}{\mathbf{C}^{\dagger}\mathbf{R}^{-1}\mathbf{C}}. \quad (8)$$

$P_{\mathrm{Cap}}(r)$ is called the Capon range profile.

This method can estimate multiple targets within a range gate when the number of targets is less than that of the dimension of $\mathbf{R}$[12].

2.3 Suppressing the coherent interference by frequency averaging

Since the data taking time of a single range gate is sufficiently short, we assumed that the target intervals were constant while receiving the echo from a range gate. When an echo from a single range gate contains multiple coherent interferences, the cross correlation between the signal from the desired distance and the coherent interference is nonzero. In this case we cannot employ an expectation process, a technique to suppress the cross correlation terms between a desired signal from interferences. Therefore we introduced an assumption to calculate the output power with a reference wave.

$$P \cong y s_{\mathrm{r}}^{*} \quad (9)$$

where s_{r}* is a reference wave.
The Capon method selects the weighting function to minimize the sum of signals, and thus results in the cancellation of the signal from the desired distance by a coherent interference. To solve this problem, we suppressed the correlation between a desired signal and coherent interferences by a frequency averaging technique. The phase relation of those signals change differently according to their respective target distances. Thus averaging the correlation at several frequencies can suppress the correlation between a desired signal and coherent interferences, i.e. frequency averaging uses the same principle as spatial averaging[12].
We defined a correlation matrix of the nth subarray $\mathbf{R}_n$ and K-element subarrays to employ a frequency averaging technique, as shown in Fig. 2. The frequency averaged correlation matrix **R'** is given by

$$\mathbf{R}' = \sum_{n=1}^{N} v_n \mathbf{R}_n \quad (10)$$

where v_n is an averaging weight for the correlation matrices of the subarrays. v_n is a real number and subject to the following equation:

$$\sum_{n=1}^{N} v_n = 1. \quad (11)$$

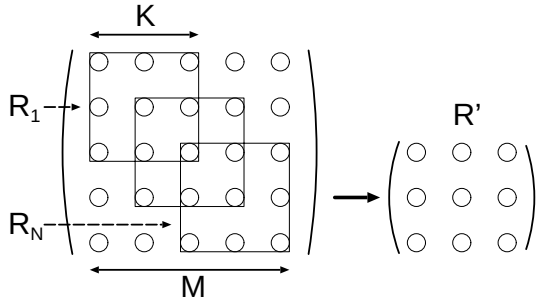

Fig. 2 The relationship between the correlation matrices of the full array and each subarray.

Two averaging techniques have been proposed for suppression of the correlation[13]. Uniform frequency averaging (UFA) averages the correlation in uniform weights. In this case, averaging weights are defined as follows;

$$v_n = \frac{1}{N}, \quad (n = 1, \cdots, N). \quad (12)$$

Adaptive frequency averaging (AFA) averages the correlation utilizing controlled weights to suppress the correlation completely. When the correlation is suppressed completely, the correlation matrix **R'** becomes a Toeplitz matrix having equal valued elements along each diagonal. Thus we set the averaging weights so as to equalize the elements in the diagonal of the averaged matrix **R'**. A measure of deviation of the correlation matrix for a Toeplitz matrix is given by

$$\varepsilon = \sum_{i=0}^{K-2} \sum_{k=1}^{K-i} \left| r_{k+i,k}' - r'(i) \right|^2, \quad (13)$$

$$r'(i) = \frac{1}{K-i} \sum_{k=1}^{K-i} r_{k+i,k}' = \frac{1}{K-i} \sum_{k=1}^{K-i} \left(\sum_{n=1}^{N} v_n r_{k+i,k,n} \right), \quad (i = 0, \cdots, K-2) \quad (14)$$

where $r_{k+i,\,k,\,n}$ is the $(k+i,\ k)$ element of $\mathbf{R}_n$. Equation (13) can be also rewritten as follows;

$$\varepsilon = \mathbf{V}^T \mathbf{R}_{ee} \mathbf{V}, \quad (15)$$

$$V = \left[v_1, v_2, \cdots, v_N \right]^{\mathrm{T}} \quad (16)$$

$$R_{ee} = \sum_{i=0}^{K-2} \sum_{k=1}^{K-i} \mathrm{Re}\{ \mathbf{e}_{k+i,k} \cdot \mathbf{e}_{k+i,k}^{\dagger} \} \quad (17)$$

$$\mathbf{e}_{k+i,k} = \left[e_{k+i,k,1}, \cdots, e_{k+i,k,n} \right]^{\mathrm{T}} \quad (18)$$

$$e_{k+i,k,n} = r_{k+i,k,n} - \frac{1}{K-i} \sum_{k=1}^{K-i} r_{k+i,k,n}, \quad (i = 0, \cdots, K-2; k = 1, \cdots, K-i; n = 1, \cdots, N) \quad (19)$$

where Re{} denotes the real part and $e_{k+i,\,k,\,n}$ is a deviation of the $(k+i,\ k)$ element of $\mathbf{R}_n$ from the mean value along its ith subdiagonal. Therefore, this problem can be expressed as follows;

$$\min \left(\varepsilon = \mathbf{V}^{\mathrm{T}} \mathbf{R}_{ee} \mathbf{V} \right) \quad \text{subject to } \mathbf{V}^{\mathrm{T}} \mathbf{I} = 1 \quad (20)$$

where $\mathbf{I}$ denotes an N-dimensional vector in which all the elements are unity. The optimum averaging weights is

$$\mathbf{V}_{\mathrm{opt}} = \mathbf{R}_{ee}^{-1} \mathbf{I} (\mathbf{I}^{\mathrm{T}} \mathbf{R}_{ee}^{-1} \mathbf{I})^{-1}. \quad (21)$$

The resolution of AFA is generally higher than that of UFA[12]. In this case this method can estimate multiple targets within a range gate when the number of targets is less than that of the dimension of **R'**.[12].

2.4 Whitening

Capon method assumes that sampled frequency components of a signal have equal transmit power. When we utilize a wideband signal for acoustic imaging, the transmit power varies with its frequency. To solve this problem we corrected the transmit power of all sampled frequency components uniformly. A frequency component of a received signal is expressed by the following equation:

$$X_l(\omega) = F(\omega) S_{\mathrm{r}}^{*}(\omega) = \left| S_{\mathrm{r}}(\omega) \right|^2 \{ a_1(\omega) \mathrm{e}^{-\mathrm{j}\omega\tau_1} + a_2(\omega) \mathrm{e}^{-\mathrm{j}\omega\tau_2} \} \quad (22)$$

where ω is the angular frequency of the lth frequency component of a received signal, $F(\omega)$ is the echo spectrum, $S_{\mathrm{r}}(\omega)$ is the reference spectrum, $a_i(\omega)$ is a parameter of the waveform change due to the ith target and τ_i is delay time in the ith target, respectively. In this study we introduced the assumption that the waveform of echoes is same as that of the reference wave. Therefore, whitening correlation spectrum $X_{\mathrm{whil}}(\omega)$ is given by

$$X_{\mathrm{whil}}(\omega) = \frac{1}{\left| S_{\mathrm{r}}(\omega) \right|^2 + \eta} X_l(\omega) = \frac{\left| S_{\mathrm{r}}(\omega) \right|^2}{\left| S_{\mathrm{r}}(\omega) \right|^2 + \eta} \{ A_1 \mathrm{e}^{-\mathrm{j}\omega\tau_1} + A_2 \mathrm{e}^{-\mathrm{j}\omega\tau_2} \}, \quad (23)$$

where η is the noise power of a received signal, A_1 and A_2 are constants, and A_1 / A_2 is the amplitude ratio of the two backscatter waves. η can be estimated from the variance of the power spectrum of a received signal when the power spectrum of the signal is uniform in a certain frequency band. Therefore the noise estimation method is not adequate for the case using a wideband signal with variation of power spectrum. We thus introduced an assumption that the expectation of the noise power is uniform, and estimated the noise power using the power spectrum of the received signal in a high frequency band, where the signal power is supposed to be zero. In this study we set the frequency band for noise estimation as 6.25 to 56.25 times the center frequency. Figure 3 shows the whitening correlation spectrum of the echo from acrylic board. Two targets time interval is 0.4 μs.

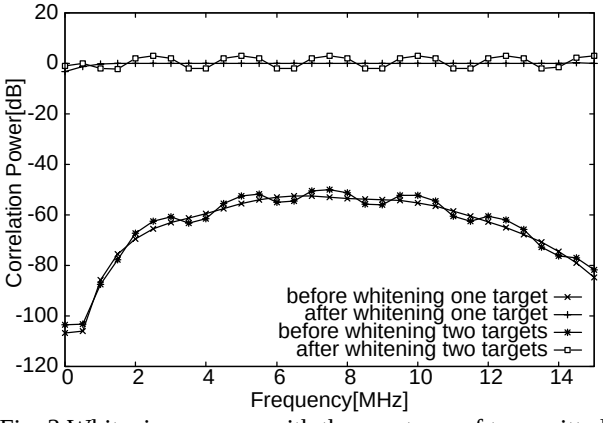

Fig. 3 Whitening process with the spectrum of transmitted signal after applying a matched filter.

3. Target detection with a single reference wave

In this section we employed a single reference wave to calculate the output power. This means that we introduced the assumption that all signals have the same waveform as that of the reference wave. First we investigated the proposed method using computational simulation. Then we examined the method experimentally.

3.1 Numerical Experiment

We evaluated the effectiveness of the proposed technique by a computational simulation using a pseudo echo. We assumed that two boundaries existed 0.05mm apart and an echo consisted of two backscatters from the two boundaries. We made the pseudo echo

$$s_1(t) = as_0(t) + bs_0(t-\tau) + n(t) \quad (24)$$

where $s_0(t)$ is the signal from an acrylic board surface shown in Fig. 4, τ is the time delay resulting from the thickness of the sheet and $n(t)$ is white noise. The parameters of the pseudo echo shown in Fig. 4 are A_1/A_2 = 0.493, τ = 0.051μs and S/N = 38.3dB. We used the echo from an acrylic board surface as a reference wave. Figure 5 shows the normalized brightness distribution of the pseudo echo given by the beamformer method, the Capon method with UFA and that with AFA. In this study, we employed 26 equally spaced frequencies within the range of 1.5 to 14.0MHz, where these frequencies have the power above -20dB of the maximum power. The beamformer method hardly detected two signals from the echo. Utilizing the Capon method, two edges were detected clearly and half power width of two edges were 1.55, 0.77μm in UFA and 1.69, 0.62μm in AFA. Estimation error in thickness was 0.92μm in UFA and 1.15μm in AFA, respectively. In the ideal case without noise, we can estimate the echo power correctly.

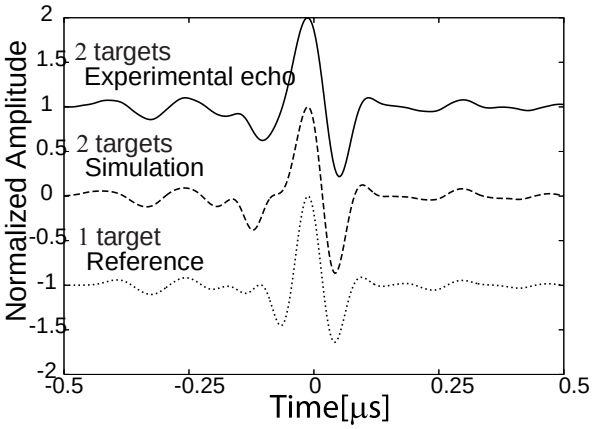

Fig. 4 The echo from a 0.05 mm thick polyethylene sheet, the pseudo echo $s_1(t)$ and the echo from an acrylic board.

3.2 Experimental study

In this section we also investigated the proposed technique experimentally. Figure 6 shows a schema of the experiment of this study. The target is a polyethylene sheet 0.05mm thick. The transmit waveform was a monocycle pulse, the center frequency was 8MHz, sampling frequency was 500MHz. The echo consisted of two backscattering waves from the front and back of the polyethylene sheet. We detected two waves from the echo using FDI with the Capon method and then estimated the thickness of the sheet.

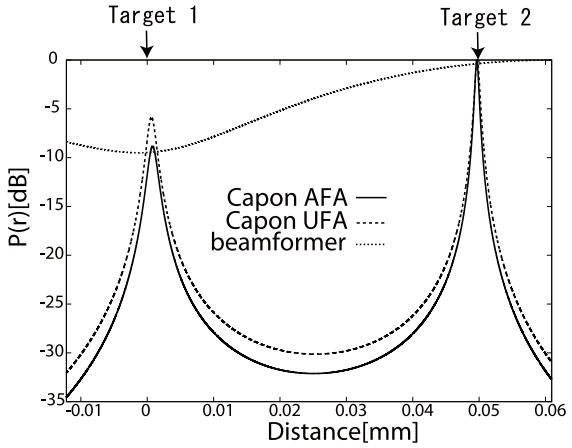

Fig. 5 The normalized brightness distribution from a pseudo echo where the two targets are located with a distance 0.05mm. Target distances are estimated using the beamformer method, the Capon method with UFA and the Capon method with AFA.

In this study we employed a echo from a polyethylene board with coherent integration of 10000 pulses, as shown in Fig. 4. The noise power of the polyethylene echo with coherent integration is 38.3dB, where the frequency band utilized for noise power estimation is 50 to 450MHz. Figure 7 shows the normalized brightness distribution calculated from the echo. In this case, we also used the echo from an acrylic board surface as a reference wave and the same parameters for imaging as those of the computational testing. It was difficult to separate the echo employing the beamformer method. Utilizing the Capon method two targets were detected, but the range resolution of the Capon method using a single reference wave deteriorated severely.

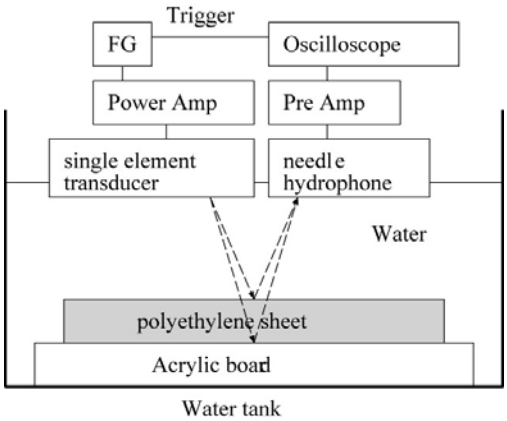

Fig. 6 Schema of the experimental setup.

4. Target detection with multiple reference waves

The frequency spectrum of an echo is particular to a target which scatters the echo. We thus employed multiple reference waves and adopted an optimum reference wave

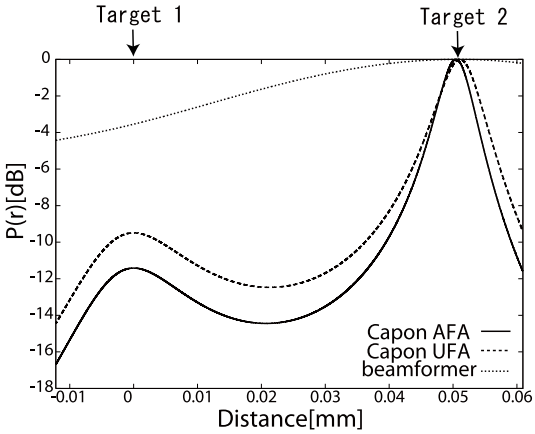

Fig. 7 Normalized brightness distribution calculated from a polyethylene sheet echo.

to each target. In this section we utilized the Capon method with UFA.

4.1 Composition of reference waves

The frequency spectrum of a signal is similar to that of other signals. Therefore we can compose a waveform similar to that of a signal from a target using several basic signals. In this paper, we employed two basic signals , an echo from an acrylic board and that from a polyethylene board, to compose reference waves. An interpolated reference wave in the frequency domain is

$$S_r(f) = \{(1-\alpha)a_1(f) + \alpha a_2(f)\} \exp\left[j\{(1-\alpha)\phi_1(f) + \alpha\phi_2(f)\}\right], \quad (25)$$

$$B_1(f) = b_1(f)\exp\left[j\phi_1(f)\right], \quad (26)$$

$$B_2(f) = b_2(f)\exp\left[j\phi_2(f)\right], \quad (27)$$

where α is an interpolation coefficient, f is a frequency, B_1 and B_2 are normalized echoes from a polyethylene board and an acrylic board in the frequency domain, respectively. Figure 8 shows the two basic waves and two interpolated reference waves used in this study. Figure 9 shows the estimated power distribution using several interpolated reference waves where the range of interpolation coefficient is 0 to 1.

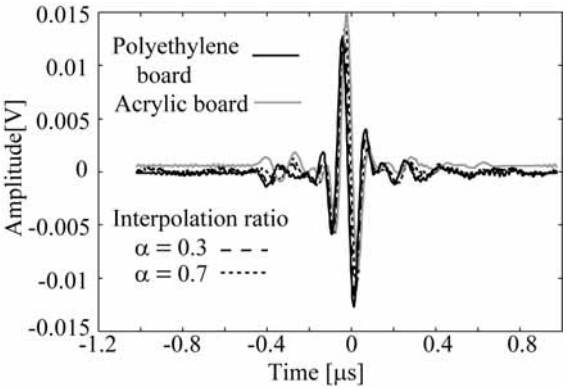

Fig. 8 Composed reference waves from two basic waves, an echo from an acrylic board and that from a polyethylene board.

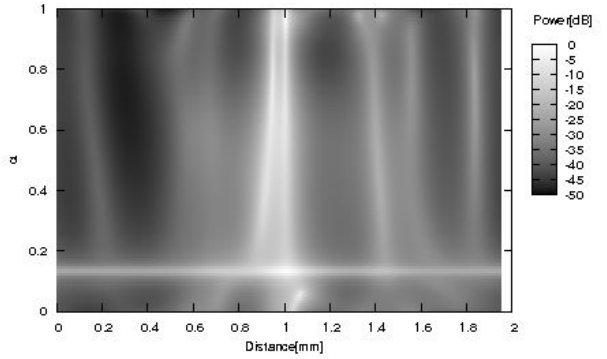

Fig. 9 Normalized estimated power distribution calculated using FDI with various interpolated reference waves. The echo consisted of two backscattering waves from the front and back of a polyethylene sheet 0.05mm thick.

4.2 Target detection using optimized reference waves

When the waveform of a reference wave is similar to that of a signal from a target, it is supposed that the estimated target position is close to the true target position. Therefore we utilized the stability of the estimated target position, i.e. the derivation of a target position with respect to the interpolation coefficient, to determine the number of targets, the approximate positions of targets, and valid interpolation coefficient values. In the case of the experiment, the deviations of two maximums of the estimated power are low when the range of interpolation coefficient is 0.3 to 1. Thus the proposed method could estimate that two targets existed and the range of valid interpolation coefficient is 0.3 to 1.

When the waveform of a reference wave is close to that of a signal from a target, it is supposed that spatial resolution around the target range becomes high. We thus set the reference wave with a minimum half power width of a estimated power distribution as the optimum reference wave at the range. In the case of the experiment, the optimum interpolation coefficient values for the front and back of a polyethylene sheet are 0.81 and 0.99, respectively. We employed a reference wave of α=0.81 to estimate power distribution around the position at the front of the sheet, and a reference wave of α=0.99 to estimate power distribution around the position at the back of the sheet. Figure 10 shows that the proposed target detection method, using two optimized reference waves, has higher spatial resolution than that using a single reference wave. An envelope method, a traditional medical acoustic imaging technique, cannot distinct two target boundaries. The half power width of the proposed method using optimized reference waves are 13μm and 6.8μm at the position of the front and back of the sheet, respectively. The results showed the effectivity of the proposed target detection method using multiple optimized reference waves.

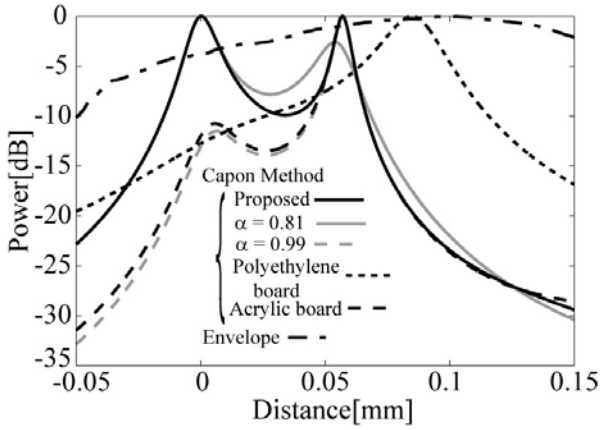

Fig.10 Normalized estimated power distribution of a signal from a polyethylene sheet 0.05mm thick. The proposed target detection method using two optimized reference waves has higher spatial resolution than that using a single reference wave.

5. Conclusions

In this paper, we proposed a medical acoustic imaging technique using FDI with the Capon method. The results of the computational testing indicated that FDI with Capon method using a single reference wave can distinct two target boundaries that lie 0.05mm apart, where the beamformer method cannot distinct when there is perfect correlation between two echoes from the boundaries. Utilizing the Capon method, half power width of two edges were 1.55, 0.77μm in UFA and 1.69, 0.62μm in AFA. Estimation error in thickness was 0.92μm in UFA and 1.55μm in AFA, respectively. In the experimental study the range resolution of FDI with Capon method using a single reference wave deteriorates severely because we approximated the auto-correlation function of the echo to the cross-correlation function of the echo and the reference signal. Therefore we proposed FDI with Capon method using multiple optimized reference waves. The proposed target detection method using optimized reference waves has higher range resolution than that using a single reference wave, and can distinct two target boundaries that lie 0.05mm apart experimentally. The half power width of the proposed method using optimized reference waves are 13μm and 6.8μm at the position of first and second target boundaries, respectively.

Acknowledgements

This work is partly supported by the Research and Development Committee Grants of the Japan Society of Ultrasonics in Medicine, Japan and the Innovative Techno-Hub for Integrated Medical Bio-imaging Project of the Special Coordination Funds for Promoting Science and Technology, from the Ministry of Education, Culture, Sports, Science and Technology (MEXT), Japan.

References

1) N. Nakagawa, H. Hasegawa and H. Kanai: *Jpn. J. Appl. Phys*. **43** (2004) 3220.
2) C. Arihara, H. Hasegawa and H. Kanai: *Jpn. J. Appl. Phys*. **45** (2006) 4727.
3) J. Inagaki, H. Hasegawa, H. Kanai, M. Ichiki and F. Tezuka: *Jpn. J. Appl. Phys*. **45** (2006) 4732.
4) K. Kudo, H. Hasegawa and H. Kanai: *Jpn. J. Appl. Phys*. **46** (2007) 4873.
5) N. Kudo, X. Zhang and K. Yamamoto: *J Med Ultrasonics*. **25** (1998) 155.
6) J. Capon: *Proc. IEEE*. **57** (1969) 1408.
7) T. J. Shan and T. Kailath: *IEEE Trans*. ASSP-**33** (1985) 527.
8) J. A. Mann and W. F. Walker: *in Proc. IEEE Ultrason. Symp*, (2002) 1807.
9) M. Sasso and C. C. Bacrie: *in Proc. IEEE*, **ICASSP** (2005) 489.
10) H. Luce, M. Yamamoto, S. Fukao, D. Helal and M. Crochet: *Journal of Atmospheric and Solar -Terrestrial Physics*. **63** (2001) 221.
11) L. Smaini, H. Luce, M. Crochet, and S. Fukao: *J. Atmos. Oceanic Technol*. **19** (2001) 954.
12) K. Takao and N. Kikuma: *IEEE Trans. Antennas Propagat*. AP-**35** (1987) 1389.
13) O. L. Frost: *IEEE ICASSP*. **86** (1986) 2499.
14) B. Van Veen and K. M. Buckley: *IEEE Trans*. ASSP-**5** (1988) 4.
15) O. L. Frost, III: *Proc. IEEE*, **60** (1972) 926.